The EMT-activator Zeb1 is a key factor for cell plasticity and promotes metastasis in pancreatic cancer

The EMT-activator Zeb1 is a key factor for cell plasticity and promotes metastasis in pancreatic cancer

Angela M. Krebs[1,2,3], Julia Mitschke[4], María Lasierra Losada[1], Otto Schmalhofer[4], Melanie Boerries[3,5], Hauke Busch[3,5], Martin Boettcher[6], Dimitrios Mougiakakos[6], Wilfried Reichardt[3,7], Peter Bronsert[3,8], Valerie G. Brunton[9], Christian Pilarsky[10], Thomas H. Winkler[11], Simone Brabletz[1], Marc P. Stemmler[1,*], Thomas Brabletz[1,*]

[1] Dept. of Experimental Medicine 1, Nikolaus-Fiebiger-Center for Molecular Medicine, FAU University Erlangen-Nürnberg, Glückstr. 6, 91054 Erlangen, Germany
[2] University of Freiburg, Faculty of Biology, Schaenzlestr. 1, 79104 Freiburg, Germany
[3] German Cancer Consortium (DKTK), Freiburg, Germany; German Cancer Research Center (DKFZ), 69121 Heidelberg, Germany.
[4] Dept. of General and Visceral Surgery, University of Freiburg Medical Center, Hugstetter Str. 55, 79106 Freiburg, Germany
[5] Systems Biology of the Cellular Microenvironment Group, Institute of Molecular Medicine and Cell Research (IMMZ), Albert-Ludwigs-University Freiburg, Germany, Stefan-Meier-Str. 17, 79106 Freiburg, Germany
[6] Dept. of Internal Medicine 5, Hematology and Oncology, Universitätsklinikum, FAU University Erlangen-Nürnberg, Ulmenweg 18, 91054 Erlangen, Germany
[7] Dept. of Radiology Medical Physics, University Medical Center, Freiburg, Breisacher Str. 60a, 79106 Freiburg, Germany
[8] Inst. of Pathology and Comprehensive Cancer Center, University Medical Center, Freiburg, Breisacher Str. 115a, 79106 Freiburg, Germany
[9] Edinburgh Cancer Research Centre, Institute of Genetics & Molecular Medicine, University of Edinburgh, Crewe Road South, Edinburgh EH4 2XR, UK
[10] Dept. of Surgery, Universitätsklinikum, FAU University Erlangen-Nürnberg, Ulmenweg 18, 91054 Erlangen, Germany
[11] Chair of Genetics, Nikolaus-Fiebiger-Center for Molecular Medicine, Dept. Biology, FAU University Erlangen-Nürnberg, Glückstr. 6, 91054 Erlangen, Germany

*both authors contributed equally and share senior authorship

*Correspondence should be addressed to T.B. (e-mail: thomas.brabletz@fau.de) or M.P.S. (e-mail: marc.stemmler@fau.de)

ABSTRACT

Metastasis is the major cause of cancer-associated death. Partial activation of the epithelial-to-mesenchymal transition (partial EMT) program was considered a major driver of tumour progression from initiation to metastasis. However, the role of EMT in promoting metastasis was recently challenged, in particular concerning effects of the Snail and Twist EMT transcription factors (EMT-TFs) in pancreatic cancer. In contrast, we show here that in the same pancreatic cancer model driven by Pdx1-cre-mediated activation of mutant *Kras* and *p53* (KPC-model) the EMT-TF Zeb1 is a key factor for the formation of precursor lesions, invasion and notably metastasis. Depletion of *Zeb1* suppresses stemness, colonisation capacity and particularly phenotypic/metabolic plasticity of tumour cells, likely causing the observed *in vivo* effects. Accordingly we conclude that different EMT-TFs have complementary and tissue-specific sub-functions in driving tumours towards metastasis. Consequently, therapeutic strategies directed at EMT-TFs, should consider such specificities and target those factors simultaneously.

Metastasis is still the major cause of cancer-associated death. Partial activation of the embryonic epithelial-to-mesenchymal transition (partial EMT) program was considered as a major driver of tumour progression from initiation to metastasis[1-3]. Most of the studies involved manipulation of different EMT-inducing transcription factors (EMT-TFs), such as Snail, Slug, Twist and ZEB1 in cell-culture or xenograft mouse models. Particularly, the EMT activator ZEB1 was shown to be important for tumourigenicity and metastasis, by triggering combined activation of cell motility and stemness properties[4-6]. However, the role of EMT in invasion and metastasis was challenged by two recent publications using genetic mouse models for breast and pancreatic cancer[7, 8]. Particularly, genetic depletion of the EMT-activators *Snai1* or *Twist1* had no effect on tumour initiation, invasion or metastasis in pancreatic cancer (PDAC) driven by Pdx1-cre-mediated activation of mutant *Kras* and *p53* (KPC-model)[8]. Therefore the authors claimed that EMT is dispensable for metastasis.
We here used the same KPC-mouse model for pancreatic cancer and conditionally ablated the EMT-activator *Zeb1* in tumour cells. In contrast to *Snai1* and *Twist1*, depletion of *Zeb1* strongly affected formation of precursor lesions, tumour grading, invasion and notably metastasis during PDAC progression. In summary we conclude that EMT is important for metastasis, but there is considerable variability and tissue specificity (and not redundancy) in the role and function of different EMT-TFs.

RESULTS

Zeb1 depletion reduces grading, invasion and distant metastasis in PDAC

KPC-mice develop metastatic pancreatic cancers with an almost 100% penetrance[9]. Of note, a fraction of cancer cells and cells in precursor lesions (PanINs) express the EMT-TF Zeb1, which was considered to be important for disease progression[10], which we could confirm (Supplementary Fig. 1a and b). To prove the role of Zeb1 in the progression towards metastasis, we generated a conditional knockout allele of *Zeb1* (*Zeb1*^{fl}) (Fig.1a). Cre-

mediated zygotic deletion of *Zeb1* phenocopied the described developmental defects of a conventional *Zeb1* knockout[11], thereby confirming its loss-of function[12]. We crossed the floxed *Zeb1* allele homozygously into KPC mice (*Pdx1-cre*;*Kras*$^{LSL.G12D/+}$;*Tp53*$^{LSL.R172H/+}$) to generate KPC;*Zeb1*$^{fl/fl}$ mice (termed KPCZ) (Fig. 1a). Progeny were born in expected ratios and showed no obvious functional defects of the pancreas. Like KPC mice, all KPCZ mice developed pancreatic cancer. Notably, no significant differences to KPC were detected for a heterozygous *Zeb1* loss (KPC;*Zeb1*$^{fl/+}$) (KPCz) (Supplementary Fig. 1c), therefore KPCz mice were merged with *Zeb1* wild type genotypes (KPC) for all analyses. Loss of Zeb1 expression in KPCZ tumour cells was confirmed by immunohistochemistry (Supplementary Fig. 1b and 2). It was associated with a reduced expression of the EMT activators Zeb2, Slug, and tentatively also Snail, but the expression frequency of Twist was maintained (Supplementary Fig. 3a). Depletion of *Zeb1* did not delay the onset and only insignificantly reduced the growth rate of primary tumours (Fig. 1b). In line with this, the number of Ki67^{+} proliferating tumour cells, as well as the spontaneous apoptotic rate and the blood vessel density did not significantly differ (Supplementary Fig. 2). However, *Zeb1* deletion strongly influenced tumour differentiation. Whereas KPC tumours were often high grade and showed a high intra- and intertumourous heterogeneity, the number of high-grade tumours in KPCZ animals was strongly reduced and the tumours displayed homogenous, mostly differentiated phenotypes (Fig. 1c,d, and Supplementary Fig. 1b and 2). Better differentiation was also associated with a significantly higher Gata6 expression (Supplementary Fig. 3b), which is a marker for higher differentiation and better clinical prognosis of human PDAC[13]. KPCZ mice showed an increased deposition of extracellular matrix (Supplementary Fig. 2). Future work will address this aspect, since the different composition of the stroma in pancreatic cancer can be associated with increased[14, 15] or reduced[16, 17] aggressiveness.

Next we analysed whether depletion of *Zeb1* affects malignant tumour progression. Primary KPCZ tumours showed markedly lower local invasion (Fig. 1d). Of note, differentiated KPC

tumours also often underwent a de-differentiation associated with upregulation of Zeb1 expression in invasive tumour cells. This was not detected in KPCZ tumours, a first sign for reduced plasticity in *Zeb1*-depleted cancer cells (Fig. 1e). A major finding was that the capacity for distant metastasis was strongly reduced in KPCZ tumours (Fig. 1f, Supplementary Table 1). Thereby the corresponding metastases showed a histology and Zeb1 expression state similar to that of the primary tumor (Fig. 1g and Supplementary Fig. 3c). In summary, *Zeb1* depletion strongly reduced progression towards highly malignant, metastatic pancreatic tumours. This is in stark contrast to depletion of *Snai1* or *Twist1* in the same model, which did not affect malignant tumour progression[8].

Zeb1 depletion reduces stemness, tumourigenic and colonisation capacities

To further investigate the consequences of *Zeb1* depletion, we isolated primary tumour cells from KPC and KPCZ mice. In agreement with the strong heterogeneity of the KPC primary tumours, corresponding tumour cells displayed highly variable phenotypes from mesenchymal, to mixed and epithelial. This was evident from the growth patterns, as well as the expression of epithelial and mesenchymal marker genes (Fig. 2a-d and Supplementary Fig. 4a). In contrast all tumour lines derived from KPCZ mice were fixed in an epithelial state with strongly reduced mesenchymal gene expression. However, despite the strong phenotypical differences between KPC and KPCZ-derived cancer cell lines, we detected no consistent difference in proliferation (Fig. 2e). Accordingly, the sensitivity to the chemotherapeutic agent gemcitabine, which targets proliferating cells, was variable, but not consistently changed between KPC and KPCZ cancer cells. This was also the case for two pancreatic cancer cell lines isolated from KPC tumours with depletion of *Snai1* (KPCS) (Supplementary Fig. 4b). KPCZ cells were tentatively more resistant to the EGFR inhibitor erlotinib, but we did not detect a significant difference between KPC and KPCS cells. Upon s.c. grafting into syngeneic mice at high injection dose (1 x 10^5 cells), all KPC and KPCZ cell

lines gave rise to tumours mimicking the differentiation state of the cell line and the growth pattern of the corresponding primary tumour, supporting the *in vitro* data on differentiation and proliferation (Supplementary Fig. 4a,c,d).

Strikingly, although all tumour cell lines did not show significant changes in proliferation and were able to grow subcutaneously, the lung colonisation capacity after intravenous injection was almost completely eradicated for all KPCZ cell lines (Fig. 3a). This was not due to differences in the capability to reach the lung, since there was no significant reduction of disseminated cancer cells in the lung (Fig. 3b and Supplementary Fig. 5a). Notably, in comparison to KPCZ lines, genetic depletion of *Snai1* (KPCS cells) had no effect on lung colonisation capacity (Fig. 3c), confirming data by Zheng et al.[8]. This goes along with considerably high, albeit varying levels of Zeb1 expression in the KPCS lines, which might explain the maintained colonisation capacity. The relevance of Zeb1 expression even at reduced levels was further demonstrated in KPC cells after partial depletion of Zeb1 to 30-50% of the original levels, which did not significantly affect the lung colonisation capacity (Fig. 3d).

Since crucial traits for distant colonisation include stemness and tumourigenicity, we tested these features. Tumourigenicity of the cell lines was significantly reduced in KPCZ cell lines, particularly when compared to the KPC cell lines with a similar epithelial phenotype (Supplementary Fig. 5b). Interestingly within the KPC cell lines the epithelial differentiated cells had a higher tumourigenic capacity compared to mesenchymal type cell lines. This is in agreement with data showing that the plasticity of re-epithelialisation is important to some degree for tumourigenic and colonisation capacity and that non-plastic mesenchymal cells do not efficiently metastasize[18-20]. In addition, depletion of *Zeb1* almost completely reduced the sphere forming capacity, a surrogate test for stemness competence (Fig. 3e and Supplementary Fig. 5c). Analysis of established marker combinations[21] for human pancreatic cancer stem cells displayed no significant differences for CD24/CD44 and CD133. Epcam,

153 another marker was not applicable, since it is a direct target of Zeb1 repression[22] and thus
154 strongly upregulated in KPCZ cells (Supplementary Fig. 5d). This is in line with data showing
155 that human PDAC stemness markers are not applicable in the KPC model[23]. However, the
156 stem cell marker Sox2 turned out to be completely absent in KPCZ cell lines and s.c. grafted
157 tumours in comparison to KPC cell lines (Fig. 3f,g). Strongly reduced Sox2 expression upon
158 *Zeb1* depletion was also reflected in the primary KPC tumours (Supplementary Fig. 2). Sox2
159 expression was proposed to be stabilized by Zeb1, through its reciprocal feedback loop with
160 miR-200 family members[24]. We confirmed this hypothesis by showing that miR-200c, which
161 is strongly upregulated in KPCZ cell lines (Fig. 2c), suppressed both *Zeb1* and *Sox2*
162 expression in KPC cell lines (Fig. 3h). These data are of particular relevance since *Sox2*
163 expression is enhanced in aggressive subtypes of human PDACs[25-27]. Together our data
164 indicate that Zeb1 increases the tumourigenic capacity and is crucial for colonisation of
165 distant organs. Moreover, depletion of *Zeb1* is again in stark contrast to a depletion of *Snai1*
166 or *Twist1*, which did not affect the tumourigenic and colonisation capacity.
167 According to this data we wondered, why we did not see an effect on the primary tumour-free
168 survival in KPCZ mice (Fig. 1b). It is known that mutant p53 boosts tumour progression by
169 inducing a mutator phenotype[28, 29]. In addition it was shown that mutant p53 overcomes a
170 growth arrest in pancreatic cancer[30]. Thus we speculated that once a precursor lesion is
171 formed, the progression towards a highly proliferating tumour is too fast to detect changes in
172 the initial tumourigenic capacity. Therefore we analysed mutant *Kras* mice without the *p53*
173 mutant allele (Pdx1-cre;$Kras^{LSL.G12D/+}$, termed KC). These mice develop slowly progressing
174 acinar-ductal metaplasia (ADM)- as well as PanIN-precursor lesions, which also express
175 Zeb1[10]. In contrast to KPCZ, KC mice with homozygous deletion of *Zeb1* (termed KCZ)
176 showed a strongly reduced number and grading of PanIN and ADM lesions (Fig. 4a,b and
177 Supplementary Fig. 6a). This data further indicates that Zeb1 triggers the tumourigenic
178 capacity in pancreatic cancer from initial development till late stage metastasis.

Zeb1 is crucial for cancer cell plasticity

Zeb1 does not affect expression of single genes or small gene clusters but thousands of genes, leading to a complete reprogramming of cells[31] and we have shown that Zeb1 exerts pleiotropic effects on many different programs and pathways[31-33]. Therefore we performed a global gene expression analysis to examine the impact of Zeb1 on cell plasticity. A principal component analysis (PCA) showed a clear separation of KPC- and KPCZ-cell lines and a separation of the epithelial and mesenchymal phenotype along the first (PC1) and second principal component (PC2), respectively (Fig. 5a). The latter verified the initial findings that a depletion of *Zeb1* fixes the cells in a homogenous epithelial state, indicating that Zeb1 is a critical factor underlying cell heterogeneity and potentially also plasticity. In line with the PCA, a gene set enrichment analysis (GSEA) confirmed that *Zeb1* depletion shifts the cells towards an epithelial phenotype (Supplementary Fig. 6b). Moreover, loss of *Zeb1* expression enriches for genes associated with addiction to *Kras* expression[34], reduced metastastic competence[35], as well as the “classical” subtype of human PDACs, which have the best clinical prognosis[36] (Fig. 5b). We further analysed the expression of genes strongly associated with metastatic progression, including *Pdgfrb*, which is essential to drive metastasis in pancreatic cancer together with mutant p53[37]. All of the analysed genes were expressed in KPC cell lines, but strongly downregulated upon *Zeb1* depletion (Fig. 5c). However, in agreement with the heterogeneous phenotypes, these pro-metastatic genes were expressed only at low levels in KPC tumour cells with epithelial differentiation, although these cell lines had the highest lung colonisation capacity. We hypothesized that epithelial KPC cells possess enough plasticity to adapt their gene expression.

Enhanced plasticity of cancer cells is considered an important driving force of malignant tumour progression by allowing continuous adaptions to the demanding conditions in the changing tumour environment[1, 38, 39]. We have previously demonstrated that ZEB1,

particularly through its feedback loop with miR-200 family members, is a motor of cellular plasticity in response to extracellular cues[4]. Thus, we hypothesized that the presence of Zeb1 allows adaptations of gene expression patterns and that loss of cellular plasticity is an important consequence of *Zeb1* depletion in cancer cells. We tested this hypothesis by treating KPCZ cells with TGFβ1, a driver of malignant tumour progression and prominent inducers of EMT[40, 41]. As expected, upon TGFβ treatment KPC cells with an epithelial phenotype underwent an EMT. However, even after long-term TGFβ treatment KPCZ cells maintained their epithelial phenotype (Fig. 6a,b and Supplementary Fig. 7a). Thus without Zeb1, the cells were locked in their phenotypic state and lost plasticity. Loss of plasticity was also reflected in TGFβ-induced changes in global gene expression, where in contrast to KPC cell lines with an epithelial phenotype, the epithelial KPCZ cell lines displayed a strongly reduced responsiveness to TGFβ (Fig. 6c). The PCA showed an induction of a mesenchymal phenotype only of the KPC cell lines under TGFβ stimulation along the first principal component (PC1). Among the 20,052 analysed genes, 1514 were significantly regulated upon long-term TGFβ treatment (Fig. 6c and Supplementary Table 2), however, 1,377 (91%) of them depended on the genetic presence of *Zeb1*. The genes associated with metastatic progression including *Pdgfrb*, which were not present in epithelial KPC cells, were also upregulated by TGFβ in a Zeb1-dependent manner (Fig. 6d). These data also indicate that Zeb1 is important for a large fraction of TGFβ induced changes. The Zeb1-dependent TGFβ induced genes also included genes, which we recently identified as common Zeb1/Yap target genes upregulated in aggressive cancer types (Supplementary Fig. 7b)[31]. The high Zeb1 dependent plasticity was further indicated by the fact that Zeb1 associated phenotypic and gene expression changes were reversible after withdrawal of TGFβ (Fig. 6e-g).

Another important aspect in cancer cell biology is metabolics. Tumour cells show a high metabolic plasticity in reacting to environmental changes on their way to metastasis[42]. We exemplified this by modulating the two basic energy consumption pathways: glycolysis and

oxidative phosphorylation (OxPhos). As measured in a mito stress test, KPCZ cells have a lower basal respiration and respiration-related ATP production as indication of reduced OxPhos (Fig.7a), which is also visible in a glycolysis stress test (Fig. 7b). Blocking of OxPhos by oligomycin in a glycolysis stress test forces cells to exploit their glycolytic capacity for fulfilling energy demands and demonstrates a considerable glycolytic reserve in KPC cells (Fig. 7b). However, this glycolytic switch was no longer possible in KPCZ cells owing to a complete lack of a glycolytic reserve. Thus, also the plasticity in switching between basic energy pathways and adapting to different oxygen availability was strongly dependent on the expression of *Zeb1*.

Finally, high phenotypic plasticity of epithelial KPC cells was also detected *in vivo* after grafting into syngeneic mice. Although they displayed a differentiated phenotype in central tumour regions, KPC tumour cells underwent a de-differentiation associated with an upregulation of Zeb1 at the invasive front. In contrast grafted KPCZ cell lines displayed no phenotypic plasticity, but were fixed in their differentiated state (Fig. 7c and Supplementary Fig. 7c). Altogether, the data indicate that Zeb1 is very important for cellular plasticity in cancer cells.

DISCUSSION

Here, we describe a key role for the EMT-TF Zeb1 in the *in vivo* progression of pancreatic cancer from early precursor lesions towards metastasis. Genetic depletion of *Zeb1* in the pancreas reduces formation of ADM and PanIN precursor lesions, undifferentiated (high grade) carcinomas, invasion and metastasis. In isolated primary cancer cell lines *Zeb1* ablation leads to loss of cellular plasticity and fixation in an epithelial phenotype, a likely cause of reduced stemness, tumourigenicity and colonisation capacities (Table 1).

Our data demonstrate that Zeb1 acts in strong contrast to the EMT-TFs Snail and Twist in pancreatic cancer. *Snai1* or *Twist1* depletion in the same KPC-model did not affect formation of PanINs, tumour differentiation, invasion, colonisation and importantly metastasis[8]. Based on their results, Zheng et al. claimed that EMT is dispensable for metastasis. However, our data favour a different interpretation and allow a more comprehensive picture of the effect of EMT-TFs in tumours. Our results point to functional differences of EMT-TFs and demonstrate that Zeb1 stimulates pancreatic tumour progression from formation of precursor lesions to late stage metastasis.

What could be the critical functions of Zeb1? Its regulatory potential is not limited to effects on a few crucial downstream target genes, but rather leads to a global reprogramming of gene expression patterns [31] and does not only control EMT but also other programs and pathways. One of the most striking consequences of *Zeb1* depletion was the almost complete inhibition of lung colonisation. We postulate two major effects of *Zeb1* inactivation as the underlying molecular mechanism: the block in cellular plasticity, considered as a major driving force of tumour progression towards metastasis and the reduction of stemness, a crucial property underlying tumourigenicity and colonisation. Enhanced plasticity of cancer cells impresses as ongoing transitions between an undifferentiated/(partial) mesenchymal and a differentiated/epithelial phenotype[1, 38, 39, 43, 44]. We here describe a central role of Zeb1 in exerting different aspects of cellular plasticity, particularly the response to TGFβ, but also to metabolic changes and changes in the *in vivo* intratumourous heterogeneity. Differentiated KPC as well as KPCZ cancer cells only expressed low levels of metastasis-associated genes. However, only KPC cells, but not KPCZ cells, were able to activate their expression upon TGFβ treatment. These genes include *Pdgfrb*, which was recently shown to be absolutely required for metastasis in *p53*-mutant pancreatic cancer[37]. As a side effect, our finding that absence of *Zeb1* strongly reduces the number of TGFβ-regulated genes

indicates that Zeb1 is important for a large part of the TGFβ response (Supplementary Table 2). Furthermore, Zeb1-linked plasticity is exemplified by its impact on central metabolic pathways. The plasticity in switching between basic energy pathways is strongly compromised in *Zeb1*-depleted cells, displaying both a reduced OxPhos and reduced glycolytic reserve, which might also be critical for the colonisation step. In addition *Zeb1* inactivation affects stemness and tumourigenic properties, supporting the view that EMT-MET dynamics also reflects the plasticity between stemness and a differentiated state[45, 46]. Particularly the strong reduction of the stem cell factor *Sox2* in KPCZ tumours and derived cell lines is of high relevance, since its expression was correlated with stemness, plasticity and progression in pancreatic and other cancer types[25-27]. Together, our data indicate that Zeb1 is crucial for cellular plasticity and stemness/tumourigenic properties in pancreatic cancer cells.

There are several potential reasons, why particularly Zeb1 is associated with cellular plasticity. Firstly, Zeb1 is linked in a reciprocal double-negative feedback loop with members of the mir-200 family, which controls a switch between an undifferentiated/stemness and a differentiated phenotype[4]. Secondly, the *Zeb1* gene itself has a poised, bivalent chromatin configuration, allowing a rapid switch between high expression in cancer stem cells (CSCs) and low expression in non-CSCs[47]. Moreover, we are beginning to understand functional differences between Zeb1 and other EMT-TFs at the biochemical level. For instance, we have described a direct interaction of ZEB1 with the Hippo-pathway effector YAP1, which is crucial for activating a common ZEB1/YAP1 target gene set important for tumour progression[31]. Genes of this target set can be activated by TGFβ in epithelial KPC cells, but not in KPCZ cells. Notably, as demonstrated here for Zeb1, also Yap1 was shown to be important for the progression through ADM towards pancreatic carcinoma[48, 49].

Zeb1-dependent gene expression signatures also point to a clinical relevance of our findings. *Zeb1* ablation associates with tumours of the 'classical subtype' of pancreatic cancer, which has the best clinical prognosis compared to other subtypes[36, 50]. These data fit to the reduced aggressiveness of KPCZ tumours and further support data showing that *Zeb1* expression correlates with more aggressive precursor lesions and poor outcome in human pancreatic cancer[24, 51, 52]. Moreover, KPCZ cells show enrichment of a gene signature associated with KRAS-addiction. Notably, in this study absence of ZEB1 was already a determinant of KRAS-dependency[34, 53]. Thus, although KRAS bears the key mutation in pancreatic cancer[54], expression of *Zeb1* might render cancer cells independent of mutant KRAS.

However, our findings also raise additional questions. Firstly, why did we not observe a significant effect of *Zeb1* depletion on primary tumour-free survival in KPCZ mice (Fig. 1b)? When we omitted the mutant p53 allele, Zeb1 was critical for the formation of Kras-driven ADM and PanIN lesions as its depletion strongly reduced their occurrence. Similar data were recently shown in the MMTV-PyMT model of breast cancer, where Snail was important for tumour initiation and progression in a p53 wild type but not p53 mutant context[55]. Thus our data support the hypothesis that in the context of mutant p53 the progression towards a highly proliferating tumour is too fast to allow detection of changes in initial tumourigenicity. Secondly, why did we detect metastases in KPCZ animals at all? The fact that *Zeb1* loss reduces the metastatic competence to approximately 30% shows that Zeb1-associated EMT and plasticity is strongly supporting metastasis. Nevertheless, it also indicates a Zeb1-independent, albeit less efficient metastasis formation, which might include a potential partial redundancy with remaining EMT-TFs, although at a significantly lower efficacy. Another explanation could be different routes to metastasis, which likely cooperate with EMT-TF dependent mechanisms to various extents. As already postulated, different routes may emerge by acquisition of additional genetic alterations driving metastasis independent of

cellular plasticity-associated traits[1, 56]. Again, mutated p53 might enhance the generation of such a genetically driven metastasis[30]. In this light, the fact that *Zeb1* depletion efficiently reduces plasticity, colonisation and metastasis even in the context of mutant p53 is remarkable and further supports the importance of Zeb1 as a crucial driver of tumour progression.

In conclusion we demonstrated that the EMT-TF Zeb1 is a key driver of pancreatic tumour progression from early tumourigenesis to late stage metastasis, underscoring the important role of EMT-activation in these processes. By contrast, Snail and Twist were shown to be dispensable for metastasis in this cancer type, indicating that EMT-TFs have specific sub-functions, which are not redundant but complementary. Non-redundant sub-functions of EMT-TFs were already described, e.g. for Zeb1 and Zeb2 in melanoma[57, 58], for Snail and Slug in breast cancer[59], as well as for Sox4[60] and Prrx1[19]. Moreover sub-functions can be tissue specific, as demonstrated by the different roles of Snail in metastasis of breast[61] and pancreatic cancer[8]. Consequently, therapeutic strategies directed at EMT-TFs, should consider these specificities and target such factors simultaneously.

ACKNOWLEDGEMENTS

We thank Britta Schlund, Eva Bauer and Jessica Pfannstiel, as well as Uwe Appelt and Markus Mroz (Core Unit Cell Sorting and Immunomonitoring, FAU Erlangen) for expert technical assistance and Rebecca Eccles for critical reading of the manuscript. We are grateful to Dieter Saur (Dept. of Internal Medicine, TU Munich, Germany) for providing the KPCS cell lines. We thank Dr. Joseph C. Wu, from Stanford University, for the MSCV-LUC_EF1-GFP-T2A-Puro plasmid. This work was supported by grants to T.B., S.B., M.B. and M.P.S. from the German Research Foundation (SFB850/A4, B2, Z1 and

DFG BR 1399/9-1, DFG 1399/10-1, DFG BR4145/1-1) and from the German Consortium for Translational Cancer Research (DKTK).

AUTHOR CONTRIBUTIONS

A.M.K. planned and performed experiments and wrote the manuscript. J.M performed mouse experiments. M.L.L. performed drug studies. O.S. generated the floxed Zeb1 allele. M.B. and H.B. performed bioinformatics analyses. M.B. and D.M. performed metabolic tests. W.R. performed MRI analyses. P.B. performed histological analyses. V.G.B. established mouse models. C.P. generated cell lines. T.H.W. performed mouse experiments. S.B. generated the floxed Zeb1 allele, planned and performed experiments. M.P.S. generated the floxed Zeb1 allele, planned and performed mouse experiments, was involved in coordination and wrote the manuscript. T.B. planned and coordinated the project, analysed data and wrote the manuscript.

COMPETING FINANCIAL INTEREST

The authors declare no competing financial interest.

REFERENCES

1. Brabletz, T. To differentiate or not — routes towards metastasis. *Nat Rev Cancer* **12**, 425-436 (2012).
2. Kalluri, R. & Weinberg, R.A. The basics of epithelial-mesenchymal transition. *J Clin Invest* **119**, 1420-1428 (2009).
3. Nieto, M.A., Huang, Ruby Y.-J., Jackson, Rebecca A. & Thiery, Jean P. EMT: 2016. *Cell* **166**, 21-45 (2016).
4. Brabletz, S. & Brabletz, T. The ZEB/miR-200 feedback loop--a motor of cellular plasticity in development and cancer? *EMBO Rep* **11**, 670-677 (2010).
5. Vandewalle, C., Van Roy, F. & Berx, G. The role of the ZEB family of transcription factors in development and disease. *Cell Mol Life Sci* **66**, 773-787 (2009).
6. Zhang, P., Sun, Y. & Ma, L. ZEB1: at the crossroads of epithelial-mesenchymal transition, metastasis and therapy resistance. *Cell Cycle* **14**, 481-487 (2015).
7. Fischer, K.R. *et al.* Epithelial-to-mesenchymal transition is not required for lung metastasis but contributes to chemoresistance. *Nature* **527**, 472-476 (2015).

8. Zheng, X. *et al.* Epithelial-to-mesenchymal transition is dispensable for metastasis but induces chemoresistance in pancreatic cancer. *Nature* **527**, 525-530 (2015).
9. Hingorani, S.R. *et al.* Trp53R172H and KrasG12D cooperate to promote chromosomal instability and widely metastatic pancreatic ductal adenocarcinoma in mice. *Cancer Cell* **7**, 469-483 (2005).
10. Rhim, Andrew D. *et al.* EMT and Dissemination Precede Pancreatic Tumor Formation. *Cell* **148**, 349-361 (2012).
11. Higashi, Y. *et al.* Impairment of T Cell Development in deltaEF1 Mutant Mice. *The Journal of Experimental Medicine* **185**, 1467-1480 (1997).
12. Brabletz, S. *et al.* Generation and characterization of mice for conditional inactivation of Zeb1. *Genesis*, doi: 10.1002/dvg.23024 (2017).
13. Martinelli, P. *et al.* GATA6 regulates EMT and tumour dissemination, and is a marker of response to adjuvant chemotherapy in pancreatic cancer. *Gut*, doi: 10.1136/gutjnl-2015-311256. (2016).
14. Laklai, H. *et al.* Genotype tunes pancreatic ductal adenocarcinoma tissue tension to induce matricellular fibrosis and tumor progression. *Nat Med* **22**, 497-505 (2016).
15. Erkan, M. *et al.* The Activated Stroma Index Is a Novel and Independent Prognostic Marker in Pancreatic Ductal Adenocarcinoma. *Clinical Gastroenterology and Hepatology* **6**, 1155-1161 (2008).
16. Özdemir, Berna C. *et al.* Depletion of Carcinoma-Associated Fibroblasts and Fibrosis Induces Immunosuppression and Accelerates Pancreas Cancer with Reduced Survival. *Cancer Cell* **25**, 719-734 (2014).
17. Rhim, Andrew D. *et al.* Stromal Elements Act to Restrain, Rather Than Support, Pancreatic Ductal Adenocarcinoma. *Cancer Cell* **25**, 735-747 (2014).
18. Tsai, Jeff H., Donaher, Joana L., Murphy, Danielle A., Chau, S. & Yang, J. Spatiotemporal Regulation of Epithelial-Mesenchymal Transition Is Essential for Squamous Cell Carcinoma Metastasis. *Cancer Cell* **22**, 725-736 (2012).
19. Ocaña, Oscar H. *et al.* Metastatic Colonization Requires the Repression of the Epithelial-Mesenchymal Transition Inducer Prrx1. *Cancer Cell* **22**, 709-724 (2012).
20. Korpal, M. *et al.* Direct targeting of Sec23a by miR-200s influences cancer cell secretome and promotes metastatic colonization. *Nat Med* **17**, 1101-1108 (2011).
21. Raj, D., Aicher, A. & Heeschen, C. Concise Review: Stem Cells in Pancreatic Cancer: From Concept to Translation. *STEM CELLS* **33**, 2893-2902 (2015).
22. Vannier, C., Mock, K., Brabletz, T. & Driever, W. Zeb1 Regulates E-cadherin and Epcam (Epithelial Cell Adhesion Molecule) Expression to Control Cell Behavior in Early Zebrafish Development. *Journal of Biological Chemistry* **288**, 18643-18659 (2013).
23. Dosch, J.S., Ziemke, E.K., Shettigar, A., Rehemtulla, A. & Sebolt-Leopold, J.S. Cancer Stem Cell Marker Phenotypes Are Reversible and Functionally Homogeneous in a Preclinical Model of Pancreatic Cancer. *Cancer Research* **75**, 4582-4592 (2015).
24. Wellner, U. *et al.* The EMT-activator ZEB1 promotes tumorigenicity by repressing stemness-inhibiting microRNAs. *Nat Cell Biol* **11**, 1487-1495 (2009).
25. Herreros-Villanueva, M. *et al.* SOX2 promotes dedifferentiation and imparts stem cell-like features to pancreatic cancer cells. *Oncogenesis* **2**, e61. doi: 10.1038/oncsis.2013.1023 (2013).
26. Sanada, Y. *et al.* Histopathologic Evaluation of Stepwise Progression of Pancreatic Carcinoma with Immunohistochemical Analysis of Gastric Epithelial

Transcription Factor SOX2: Comparison of Expression Patterns between Invasive Components and Cancerous or Nonneoplastic Intraductal Components. *Pancreas* **32**, 164-170 (2006).
27. Singh, S.K. *et al.* Antithetical NFATc1–Sox2 and p53–miR200 signaling networks govern pancreatic cancer cell plasticity. *The EMBO Journal* **34**, 517-530 (2015).
28. Muller, Patricia A.J. & Vousden, Karen H. Mutant p53 in Cancer: New Functions and Therapeutic Opportunities. *Cancer Cell* **25**, 304-317 (2014).
29. Rivlin, N., Koifman, G. & Rotter, V. p53 orchestrates between normal differentiation and cancer. *Seminars in Cancer Biology* **32**, 10-17 (2015).
30. Morton, J.P. *et al.* Mutant p53 drives metastasis and overcomes growth arrest/senescence in pancreatic cancer. *Proceedings of the National Academy of Sciences* **107**, 246-251 (2010).
31. Lehmann, W. *et al.* ZEB1 turns into a transcriptional activator by interacting with YAP1 in aggressive cancer types. *Nat Commun* **7**, doi: 10.1038/ncomms10498 (2016).
32. Mock, K. *et al.* The EMT-activator ZEB1 induces bone metastasis associated genes including BMP-inhibitors. *Oncotarget* **6**, 14399-14412 (2015).
33. Brabletz, S. *et al.* The ZEB1/miR-200 feedback loop controls Notch signalling in cancer cells. *EMBO J* **30**, 770-782 (2011).
34. Singh, A. *et al.* A Gene Expression Signature Associated with "K-Ras Addiction" Reveals Regulators of EMT and Tumor Cell Survival. *Cancer Cell* **15**, 489-500 (2009).
35. Nakamura, T., Fidler, I.J. & Coombes, K.R. Gene Expression Profile of Metastatic Human Pancreatic Cancer Cells Depends on the Organ Microenvironment. *Cancer Research* **67**, 139-148 (2007).
36. Collisson, E.A. *et al.* Subtypes of pancreatic ductal adenocarcinoma and their differing responses to therapy. *Nat Med* **17**, 500-503 (2011).
37. Weissmueller, S. *et al.* Mutant p53 Drives Pancreatic Cancer Metastasis through Cell-Autonomous PDGF Receptor β Signaling. *Cell* **157**, 382-394 (2014).
38. Diepenbruck, M. & Christofori, G. Epithelial–mesenchymal transition (EMT) and metastasis: yes, no, maybe? *Current Opinion in Cell Biology* **43**, 7-13 (2016).
39. Ye, X. & Weinberg, R.A. Epithelial–Mesenchymal Plasticity: A Central Regulator of Cancer Progression. *Trends in Cell Biology* **25**, 675-686 (2015).
40. Bellomo, C., Caja, L. & Moustakas, A. Transforming growth factor [beta] as regulator of cancer stemness and metastasis. *Br J Cancer* **115**, 761-769 (2016).
41. Korpal, M. & Kang, Y. Targeting the transforming growth factor-β signalling pathway in metastatic cancer. *European Journal of Cancer* **46**, 1232-1240 (2010).
42. Lehuédé, C., Dupuy, F., Rabinovitch, R., Jones, R.G. & Siegel, P.M. Metabolic Plasticity as a Determinant of Tumor Growth and Metastasis. *Cancer Research* **76**, 5201-5208 (2016).
43. Nieto, M.A. Epithelial Plasticity: A Common Theme in Embryonic and Cancer Cells. *Science* **342**, doi: 10.1126/science.1234850. (2013).
44. Brabletz, T. *et al.* Variable beta-catenin expression in colorectal cancer indicates a tumor progression driven by the tumor environment. *Proc Natl Acad Sci U S A* **98**, 10356-10361 (2001).
45. Chaffer, C.L. *et al.* Normal and neoplastic nonstem cells can spontaneously convert to a stem-like state. *Proceedings of the National Academy of Sciences* **108**, 7950-7955 (2011).
46. Puisieux, A., Brabletz, T. & Caramel, J. Oncogenic roles of EMT-inducing transcription factors. *Nature cell biology* **16**, 488-494 (2014).

47. Chaffer, Christine L. *et al.* Poised Chromatin at the ZEB1 Promoter Enables Breast Cancer Cell Plasticity and Enhances Tumorigenicity. *Cell* **154**, 61-74 (2013).
48. Gruber, R. *et al.* YAP1 and TAZ Control Pancreatic Cancer Initiation in Mice by Direct Up-regulation of JAK–STAT3 Signaling. *Gastroenterology* **151**, 526-539 (2016).
49. Zhang, W. *et al.* Downstream of Mutant KRAS, the Transcription Regulator YAP Is Essential for Neoplastic Progression to Pancreatic Ductal Adenocarcinoma. *Science Signaling* **7**, ra42-ra42 (2014).
50. Moffitt, R.A. *et al.* Virtual microdissection identifies distinct tumor- and stroma-specific subtypes of pancreatic ductal adenocarcinoma. *Nat Genet* **47**, 1168-1178 (2015).
51. Galvan, J.A. *et al.* Expression of E-cadherin repressors SNAIL, ZEB1 and ZEB2 by tumour and stromal cells influences tumour-budding phenotype and suggests heterogeneity of stromal cells in pancreatic cancer. *Br J Cancer* **112**, 1944-1950 (2015).
52. Bronsert, P. *et al.* Prognostic significance of Zinc finger E-box binding homeobox 1 (ZEB1) expression in cancer cells and cancer-associated fibroblasts in pancreatic head cancer. *Surgery* **156**, 97-108 (2014).
53. Singh, A. & Settleman, J. EMT, cancer stem cells and drug resistance: an emerging axis of evil in the war on cancer. *Oncogene* **29**, 4741-4751 (2010).
54. Eser, S., Schnieke, A., Schneider, G. & Saur, D. Oncogenic KRAS signalling in pancreatic cancer. *Br J Cancer* **111**, 817-822 (2014).
55. Ni, T. *et al.* Snail1-dependent p53 repression regulates expansion and activity of tumour-initiating cells in breast cancer. *Nat Cell Biol* **18**, 1221-1232 (2016).
56. Turajlic, S. & Swanton, C. Metastasis as an evolutionary process. *Science* **352**, 169-175 (2016).
57. Caramel, J. *et al.* A Switch in the Expression of Embryonic EMT-Inducers Drives the Development of Malignant Melanoma. *Cancer Cell* **24**, 466-480 (2013).
58. Denecker, G. *et al.* Identification of a ZEB2-MITF-ZEB1 transcriptional network that controls melanogenesis and melanoma progression. *Cell Death Differ* **21**, 1250-1261 (2014).
59. Ye, X. *et al.* Distinct EMT programs control normal mammary stem cells and tumour-initiating cells. *Nature* **525**, 256-260 (2015).
60. Tiwari, N. *et al.* Sox4 Is a Master Regulator of Epithelial-Mesenchymal Transition by Controlling Ezh2 Expression and Epigenetic Reprogramming. *Cancer Cell* **23**, 768-783 (2013).
61. Tran, H.D. *et al.* Transient SNAIL1 Expression Is Necessary for Metastatic Competence in Breast Cancer. *Cancer Research* **74**, 6330-6340 (2014).

FIGURE LEGENDS

Figure 1: *Zeb1* depletion reduces invasion and metastasis in pancreatic cancer.

(a) Scheme of the genetic mouse models for pancreatic cancer. The colour code (blue KPC, red KPCZ) is used for all results. **(b)** Tumour-free survival (n= 28 KPC, 18 KPCZ; Log-rank (Mantel-Cox) test), tumour volume (0 = start of MRI measurements; n=23 KPC,

27 KPCZ; error bars show mean ±S.E.M.; multiple t-tests with correction for multiple comparison using the Holm-Sidak method). n.s. = not significant. **(c)** Representative HE-stained sections for the grading of the respective tumours. Scale bar, 250 µm and 125 µm for higher magnifications. (n=48 KPC, 29 KPCZ independent tumours) **(d)** Grading and local invasion of the respective tumours (n=48 KPC, 29 KPCZ independent tumours; error bars show mean ±S.D.; Mann-Whitney test (two-tailed), Chi-square test (two-tailed) for grade3/4 tumours), ****p<0.0001. **(e)** Representative immunohistochemical stainings of consecutive sections showing nuclear Zeb1 in tumour cells (arrows) of invasive tumour regions in KPC, but not in KPCZ mice. Asterisks mark Zeb1 expression in stromal cells, cen (central) and inv (invasive tumour regions). n= 15 KPC, 13 KPCZ independent tumours, Scale bar, 75 µm. **(f)** Numbers and grading of metastasized tumours (n=52 KPC, 29 KPCZ independent tumours; error bars mean ±S.D.; Chi-square test (two-tailed) for metastasis, Mann-Whitney test (two-tailed) for grading). **(g)** Representative images of differentiated (KPC and KPCZ) and undifferentiated (KPC) primary tumours (PT) and corresponding metastases (Met) with the same phenotype (L= liver). n= 19 KPC, 4 KPCZ independent tumours and corresponding metastases. Scale bar, 150 µm.

Figure 2: Depletion of *Zeb1* affects phenotypic variability of tumour cells.
(a) Anti-E-cadherin and anti-vimentin immunofluorescence stainings showing variable expression in KPC cell lines and homogeneous E-cadherin and lack of vimentin expression in all KPCZ cell lines. Scale bar, 100 µm. **(b)** Relative mRNA expression levels of indicated marker genes in the isolated tumour cells. **(c)** Relative mRNA expression levels for EMT transcription factors and epithelial microRNAs. mRNA levels of the cell line 661 was set to 1. n=3 biologically independent experiments, error bars mean ±S.E.M. *p<0.05, **p<0.01, n.s. = not significant, Mann-Whitney test (one-tailed) (b-c). **(d)** Immunoblots of indicated marker genes (unprocessed scans of immunoblots are shown in Suppl. Fig. 8). **(e)** BrdU proliferation assay for the isolated tumour cell lines. n=3 biologically independent experiments, error bars mean ±S.E.M. The colour code for the isolated cell lines as depicted in b) is valid for all corresponding results.

Figure 3: Depletion of *Zeb1* affects stemness, tumourigenic and colonisation capacities.

(a) Representative images of macroscopic and HE-stained lungs, 18 days after i.v. injection of tumour cells in syngeneic mice. Quantification of lung colonies (left, cell lines grouped by genotype; right, individual cell lines (for a,b,c,e), normalised to 20 mm^2 lung area). n=3mice/cell line, n=4 mice for line 524, error bars mean ±S.D.; ****p<0.0001, Mann-Whitney test (two-tailed), Scale bar, 200 µm. **(b)** No. of GFP+ cells per visual field 2 h after i.v. injection. n=3 mice/cell line, error bars mean ±S.D. Mann-Whitney test (two-tailed). **(c)** Quantification after i.v. injection of KPC, KPCS and KPCZ tumour cells in nude mice; n=13 mice for KPC, n=8 for KPCS, n=6 for KPCZ- 4 mice/cell line, Mann-Whitney test (two-tailed), **p<0.01, n.s. = not significant. Relative mRNA expression levels in KPCS cell lines; mRNA levels of KPC661 (expressing low levels of Snail) set to 1; average of n=2 biologically independent experiments, error bars mean ±S.D. Immunoblot for the indicated proteins with KPC701 as control expressing high Snail levels. **(d)** Number of lung colonies after i.v. injection of KPC shcontrol (ctr) and KPC shZeb1 tumour cells in nude mice (normalized to 20 mm^2 lung area). n= 3 mice/cell line, error bars mean ±S.D.; Mann-Whitney test (two-tailed), n.s = not significant. Immunoblots and corresponding quantifications, showing shRNA-mediated partial reduction of Zeb1. n=3 biologically independent experiments, error bars mean ±S.E.M.; unpaired Student's t-test (two-tailed)**,** **p<0.01. **(e)** Quantification of sphere forming capacity. n=3 biologically independent experiments, error bars mean ±S.D.; *p<0.05, Mann-Whitney test (two-tailed). **(f)** Relative mRNA expression levels and immunoblots of stem cell genes. mRNA levels of the line 661 set to 1. n=3 biologically independent experiments, error bars mean ±S.E.M. *p<0.05, Mann-Whitney test (one-tailed). **(g)** HE and immunohistochemical staining for Sox2 in tumours grown subcutaneously (s.c.) (n=51) or in the lung (n=36) after i.v. injection (l.c.) of indicated cell lines. Scale bar, 100 µm. **(h)** Immunoblot for indicated proteins upon overexpression of *Mir200c*. Source data for Fig. 3c, d, f see Supplementary Table 5; unprocessed scans of immunoblots are shown in Suppl. Fig. 8.

Figure 4: Depletion of *Zeb1* reduces ADM and PanIN precursor lesions.

(a-b) Consecutive sections of representative HE and PAS stained sections showing precancerous PanIN (a) and ADM lesions (b) in the pancreas of 6 month old KC and KCZ mice. Specific dark blue/purple PAS staining indicates the mucin-rich PanIN lesions, arrows indicate ADMs. Squares mark the magnified regions; Scale bars 1 mm and 150 µm for higher magnifications in (a) and 75 µm in (b). Quantification of the ADM

and PanIN areas and PanIN grading is given. n=12 KC and 7 KCZ independent mice, error bars mean ±S.D.; **p<0.01, ****p<0.0001 unpaired Student's t-test (two-tailed) with Welch's correction for ADM and PanIN areas and Mann-Whitney test (two-tailed) for grading.

Figure 5: Depletion of *Zeb1* reduces phenotypic variability

(a) Principal component analysis (PCA) of the KPC and KPCZ cell line transcriptomes. The plot depicts the first two principal components using all samples accounting for ~44%, ~17% of the variance, respectively. **(b)** Gene set enrichment analyses (GSEA) of transcriptome data from KPCZ vs. KPC cells reveal enrichment of gene signatures associated with Kras dependency and the classical type of pancreatic cancer, as well as a reduction of genes associated with metastasis in KPCZ cell lines. NES=normalized enrichment score; FDR=false discovery rate. **(c)** Relative mRNA expression levels (qRT-PCR) and immunoblots of indicated genes associated with metastasis in the isolated tumour cells. mRNA levels of the cell line 661 was set to 1. n=3 biologically independent experiments, error bars mean ±S.E.M. *p<0.05, **p<0.01, Mann-Whitney test (one-tailed). Unprocessed scans of immunoblots are shown in Suppl. Fig. 8.

Figure 6: Depletion of *Zeb1* reduces TGFβ-induced cellular plasticity.

(a) E-cadherin and vimentin immunofluorescence staining of two epithelial KPC and two KPCZ cancer cell lines treated with TGFβ1 for 3 and 21 days. Scale bar, 100 µm. **(b)** Immunoblots for indicated marker genes of the same lines as in a). Unprocessed scans of immunoblots are shown in Suppl. Fig. 8. **(c)** PCA of transcriptome signatures of the KPC and KPCZ cell lines upon TGFβ treatment. TGFβ -induced shifts in expression of the cell lines shown in a) are marked with coloured boxes (microarrays performed in duplicates, referred to as TGFβ_1 and TGFβ_2). Note, a great shift for KPC cell lines towards a mesenchymal pattern but not for KPCZ lines(upper panel). Venn diagram showing number of significantly up-or downregulated genes (cut-off: adj. p-value<0.05 and $\log_2$FC>0.5) by 14 days of TGFβ treatment of cell lines shown in a). Moderated t-test (lower panel). **(d)** Relative mRNA expression levels (qRT-PCR) of indicated genes (including the metastasis set in Fig. 5c) in KPC and KPCZ cell lines treated for different times with TGFβ (time points: 0, 6 h, 1, 3, 7, 14, 21 days). mRNA levels of the cell line 661 at day 0 were set to 1. n=3 biologically independent experiments, error bars mean

±S.E.M. Statistical analysis is shown for the comparison of TGFβ treated and untreated samples (grey bars) of each individual cell line *p<0.05, **p<0.01, unpaired Student's t-test (one-tailed). **(e)** Anti-E-cadherin and anti-vimentin immunofluorescence staining of two epithelial KPC and two KPCZ cancer cell lines treated with TGFβ for more than 21 days followed by 14 days TGFβ withdrawal. Scale bar, 100 µm. **(f-g)** Immunoblots (f) and relative mRNA expression levels (qRT-PCR) (g) of indicated marker genes of the same cell lines as in e). mRNA levels of the cell line 661 at day 0 were set to 1. n=3 biologically independent experiments, error bars mean ±S.E.M.; *p<0.05, **p<0.01, ***p<0.001, unpaired Student's t-test (one-tailed). Source data for Fig. 5d,f see Supplementary Table 5; unprocessed scans of immunoblots are shown in Suppl. Fig. 8.

Figure 7: Depletion of *Zeb1* reduces metabolic and phenotypic plasticity.
(a) Mito stress test (MST) showing the oxygen consumption rate (OCR) as indicator for oxidative phosphorylation and deduced levels for basal respiration and ATP production. **(b)** Glycolysis stress test (GST) showing the extracellular acidification rate (ECAR) as indicator for glycolysis and the OCR after glucose stimulation, blocking of oxidative phosphorylation with oligomycin and blocking of glycolysis with 2-deoxy-glucose (2DG), as well as deduced glycolytic capacity and glycolytic reserve. Note a complete lack of a glycolytic reserve (upper arrow) after blocking oxidative phosphorylation (lower arrow) in KPCZ cells. KPC661 and 792 as well as all KPCZ cell lines were used. n=7 biologically independent experiments; error bars ±S.E.M. for MST and GST and ±S.D. for other parameters; for MST and GST a multiple t-test with correction for multiple comparison using the Holm Sidak method was used; for other parameters an unpaired Students's t-test (two-tailed) was used; *p<0.05, **p<0.01, ***p<0.001, ****p<0.0001. **(c)** Representative images of consecutive sections of immunohistochemical stainings for Ck19 and Zeb1 comparing the plasticity of Zeb1 expression in central and invasive tumour regions. Shown are tumours derived from one KPC and one KPCZ cell line. Asterisks label Zeb1 expression in stromal cells, arrows indicate Zeb1-positive tumour cells at the invasive front. Ck19 expression is shown to identify cancer cells. n= 15 KPC, 13 KPCZ independent tumours, Scale bars, 50 µm and 150 µm for higher magnifications.

Table 1: Summary of the differential behaviour of KPC vs. KPCZ cell lines concerning crucial traits for tumour progression towards metastasis.

Table summarizing the experimental results of the differential behaviour of KPC vs. KPCZ cell lines concerning crucial traits for tumour progression towards metastasis. For experimental data on sphere formation see Figs. 3e, Suppl. Fig. 5c; tumorigenicity see Suppl. Fig. 5b; plasticity see Figs. 6 and 7, Suppl. Fig. 7a,c; lung colonisation see Fig. 3a; lung dissemination see Fig. 3b, Suppl. Fig. 5a. (-, no capacity; +, weak capacity; ++, moderate capacity; +++, strong capacity; na, not analysed).

METHODS

Ethic statement

Animals were kept on a 12:12 h light-dark cycle and provided with food and water ad libitum. Animal husbandry and all experiments were performed according to the European Animal Welfare laws and guidelines. The protocols were approved by the committee on ethics of animal experiments of the states Baden-Württemberg and Bavaria (Regierungspräsidium Freiburg and Regierung Unterfranken, Würzburg).

Mice

The *Pdx1-Cre* transgene (Tg(Pdx1-cre)6Tuv), the conditional *Kras*$^{LSL.G12D}$ (Kras^{tm4Tyj}) , *Tp53*$^{LSL.R172H}$ (Trp53^{tm2Tyj}) and GFP (Z/EG; Tg(CAG-Bgeo/GFP)21Lbe) alleles and the KPC mouse model have been described[9, 62-66] and were kept on a C57BL/6 background. The generation of the conditional *Zeb1* knockout allele (*Zeb1*^{fl}) is described elsewhere[12]. In brief, exon6 was flanked by loxP sites to remove sequences coding for large parts of the protein and to induce a premature translational stop. Tumour mice were generated by breedings of *Pdx1-Cre* with *Kras*$^{LSL.G12D/+}$;*Tp53*$^{LSL.R172H/+}$ mice (KPC) and *Pdx1-Cre;Zeb1*$^{fl/fl}$ with *Kras*$^{LSL.G12D/+}$;*Tp53*$^{LSL.R172H/+}$*;Zeb1*$^{fl/fl}$ mice (KPCZ). KPC and KPCZ offspring was palpated weekly for tumour initiation and enrolled for MRI measurements when tumours were identified. KC and KCZ mice (*Tp53*$^{+/+}$ genotype) were analysed with 6 months of age. Once the tumour reached a maximum tolerated size (tumour diameter of 1 cm), mice were sacrificed, perfused and organs, tumour and macroscopic metastases were isolated. Animals, which died or were sacrificed due to non-pancreatic tumour reasons (mainly growth of skin papilloma) were excluded from the analyses. Tissue was fixed in 4% paraformaldehyde (PFA) or snap frozen in TissueTek. A summary of basic tumour mice data is shown in Supplementary Table 1.

MRI

Mice were analysed with a Brucker Bio Spin 94/20, 9.4Tesla – 400MHz – 20cm small animal MR using coronal and transverse scans with a spatial resolution of 117 µm x 117 µm/pixel and a 256 x 256 matrix. Slice distance was set to 0.5 mm. Measurements were repeated weekly. Tumour volume was approximated by π/6 x l x w x d. Initial detection of a tumour after a series of tumour-free MRI measurements was defined as time-point of tumour initiation. For analysis of tumour growth curves all mice were adjusted to a tumour size of 50 mm^3.

Histology, histopathology and immunohistochemistry

PFA-fixed tissues were embedded into paraffin, sectioned at 4-5µm and stained with Mayer's Haematoxylin and Eosin solution G (HE). For histopathological scoring, tumours were classified using the standard pathological grading scheme into either well differentiated (grade 1), moderately differentiated (grade 2), poorly differentiated (grade 3) and anaplastic or sarcomatoid (grade 4). The histological invasion score was scored from no invasion (0) to high invasion (2), with invasion defined as number and distance of tumour cells disseminated from the main tumour mass. Masson's trichrome staining (MTS) was performed according to the manufacturer's instructions (Sigma-Aldrich, HT15) and counterstained by Weigert's Iron Haematoxylin. Tumour stroma composition was scored either based on MTS or HE staining for intensity of extracellular matrix deposition on a scale from 0-4. KC and KCZ pancreata were stained by alcian blue-periodic acid/Schiff's (PAS) reagent. Scoring for CD31 and Gata6 was done according to staining intensity with no (0), low (1), medium (2) and high (3) expression. PanINs were classified using the standard pathological grading score from 1-3. The complete numbers of PanINs and ADMs was counted on at least four independent tumour sections and normalized to a tissue area of 20 mm^2. In addition to macroscopic metastases, lungs and livers were screened for metastases identified by screening four series of HE stained sections separated by at least 200 µm.

Immunohistochemical analysis was performed as previously described[31]. Primary antibodies against the following proteins were used: polyclonal rabbit anti-Zeb1 (Novus Biological, NBP1-05987, 1:250); polyclonal rabbit anti-Zeb2 (Novus Biological, NBP1-82991, 1:200); monoclonal rabbit anti-Snail (Cell Signaling, #3879, Clone C15D3, 1:200); monoclonal rabbit anti-Slug (Cell Signaling, CS9585, Clone C19G7, 1:150); polyclonal goat anti-Twist (Abcam, ab50581, 1:500); polyclonal goat anti-Gata6 (R&D, AF1700, 1:1500); monoclonal mouse anti-E-Cadherin (BD Transduction Laboratories, 610182, Clone 36, 1:350); monoclonal rabbit anti-CD31 (Santa Cruz, sc-1506, Clone M-20, 1:50); monoclonal rabbit anti-Ki67 (Abcam, ab16667, Clone SP6, 1:300); monoclonal rabbit anti-cleaved Caspase 3 (Cell Signaling, CS9664, Clone 5A1E, 1:1,000); monoclonal rat anti-KRT19 (TROMA-3 hybridoma supernatant,1:20, a kind gift from Rolf Kemler); polyclonal rabbit anti-Sox2 (Abcam, ab97959, 1:1,000) and counterstained with Mayer's Haematoxylin. For Zeb1 immunofluorescence staining, cryosections were fixed in 4% PFA for 10 min, then permeabilised for 10 min in 0.25% Triton-X100/PBS. After blocking in 3% BSA/PBS, tissue was incubated with anti-Zeb1 antibody (Sigma, HPA027524, 1:100) followed by Alexa594-conjugated secondary antibody (Life technologies). All images were acquired on a Leica DM5500B microscope and a 2D deconvolution was performed when appropriate. No statistical method was used to predetermine sample size and the experiments were not randomized. Histological analyses were performed by two independent pathologists. The Investigators were not blinded to allocation during experiments and outcome assessment. Each demonstrated IHC and IF image was representative for minimum five or more cases (tumours) of indicated subtype.

Primary cell lines

A small piece of primary tumour was dissected, minced with a scalpel and plated on 6-well plates in DMEM (Gibco, 31966)/ 10%FBS (Gibco, 10500)/ 1%P/S (Gibco, 15140) at 37°C/5% CO_2 in a humidified incubator. Tumour cells that attached to the plate and grew out were passaged for generation of cell lines. Successful and complete recombination of cell line

deprivation was confirmed by PCR. KPCS cells were obtained from Dieter Saur (Dept. of Internal Medicine, TU Munich, Germany) and generated from the same KPC mouse model that additionally carried a homozygous *Snai1* deletion[67]. For partial knockdown of *Zeb1,* cells were infected with lentivirus containing a pGIPZ shZeb1 knockdown (V2LMM_18639) or a pGIPZ non-silencing shRNA control construct. Puromycin resistant GFP medium/high cells were used. Zeb1 protein expression was normalized to β-actin levels using BioRad ImageLab Software to calculate knockdown efficiencies. Induction of EMT in primary tumour cell lines was performed by adding 5 ng/ml TGFβ1 (PeproTech, 100-21) and replacing the medium daily for the duration of the experiment. miRNA overexpression was performed as previously described[31]. For FACS analysis of cancer stem cells markers $1x10^6$ cells were incubated with a combination of monoclonal rat anti-CD24-PE (BD, 553262, Clone M1/69, 1:200), monoclonal rat anti-CD44-APC (BD, 561862, Clone IM7, 1:100) and monoclonal rat anti-Epcam-FITC (ebioscience, 11-5791, Clone G8.8, 1:200) antibodies and analysed in a BD Cytoflex using CytExpert software. A total of 10,000 vital cells were counted. All studies were performed on cells cultured for less than 30 passages. All experiments using primary cells in vitro were done at least in triplicates (n=3). Only primary cells from mouse tumours were used and these were not further authenticated nor tested for mycoplasma contamination.

Immunoblotting, RNA isolation and quantitative RT-PCR

Protein was extracted with RIPA buffer and Western blotting was carried out as described[31, 32] with the exception that protein detection on the nitrocellulose membrane was done by incubation in Western Lightning Plus-ECL (Perkin Elmer, NEL103001EA) or SuperSignal West Femto Maximum Sensitivity Substrate (Thermo Scientific, 34095) and a ChemiDoc imaging system (BioRad). Antibodies against the following proteins were used: polyclonal rabbit anti-Zeb1 (Sigma, HPA027524, 1:5000); monoclonal rabbit anti-Snail (Cell Signaling, #3879, Clone C15D3, 1:1000); monoclonal mouse anti-E-Cadherin (BD Transduction

Laboratories, 610182, Clone 36, 1:5000); monoclonal mouse anti-N-Cadherin (BD Transduction Laboratories, 610920, Clone 32, 1:1,000); monoclonal rabbit anti-Vimentin (Cell Signaling, CS5741, Clone D21H3, 1:5,000); monoclonal mouse anti-ß-actin (Sigma, A5441, Clone AC-15, 1:10,000); polyclonal rabbit anti-Sox2 (Novus Biological, NB110-37235, 1:3,000); monoclonal mouse anti-Bmi1 (Millipore, 05-673, Clone F6, 1:300); monoclonal rabbit anti-PDGFRß (Cell Signaling, CS3169, Clone 28E1, 1:1,000); monoclonal rabbit anti-Sparc (Cell Signaling, CS8725; Clone D10F10, 1:1,000); monoclonal mouse anti-α-tubulin (Sigma, T6199, Clone DM1A, 1:5000). Western blots were done for at least three individual experiments and one representative blot is shown.

Total RNA was isolated and reversely transcribed using the RNeasy Plus Mini Kit (Qiagen, 74136) and the RevertAid First Strand cDNA Synthesis Kit (Thermo, K1622) for mRNA and the miRCURY universal cDNA synthesis kit II (Exiqon, 203301) for miRNA. mRNA transcripts were detected by using cDNA from 7.5 ng total RNA with 300 nM gene-specific primers, the Universal Probe Library (Roche, 04869877001) and the TaqMan Universal Master Mix (4440040, Applied Biosystems) in a 12 µl volume. miRNAs were analysed with the miRCURY ExiLENT SYBR Green Kit (Exiqon, 203421) with specific primer sets (Exicon) according to the manufacturer's instructions. All samples were run in a LightCycler 480 (Roche) and values were normalised to *Gapdh* and *Mir16-1* levels where appropriate and expressed relative to controls. For primer sequences and miR primer set details see Supplementary Table 3.

Cell viability (MTT) and BrdU cell proliferation assays

Cell viability upon gemcitabine (Sigma, G6423; ranging from 0.78 to 1000 nM) and erlotinib treatment (Cell Signaling, 5083 or Selleckchem, S1023, ranging from 0.2 to 51.2 µM) was analysed by plating 6,000 cells in 96- or 48-well plates and measured after 72 h of treatment using 5 mg/ml MTT (methylthiazolyldiphenyl-tetrazolium bromide; Sigma, M2128) as described[68]. IC50 values were calculated with GraphPad Prism using logarithmic transformed

data and nonlinear regression. For proliferation analysis 1,000 cells were plated in 96-well plates and BrdU incorporation was measured after a 2-h pulse with BrdU using the Cell Proliferation ELISA Kit (Roche, 11647229001) according to the manufacturer's instructions.

Sphere assay

For detecting sphere forming capacity, cells were resuspended as single cell suspension in serum-free DMEM/F12 medium (Gibco, 31331), containing 1% methylcellulose (Sigma, M0512), 20 ng/ml human EGF (R&D Systems, 236-EG), 20 ng/ml human FGF (BD biosciences, 354060), B27 supplement (1:50, Invitrogen, 17504), N2 supplement (1:100, Gibco, 17502), and 1% P/S. 500 single cells were seeded into individual wells of a poly(2-hydroxyethylmetacrylate)-coated (Sigma, P3932) 96-well plates. Colonies with a diameter of >80 µm were counted after 12 days.

Immunofluorescence staining

Immunofluorescence labelling was performed as described previously[31]. Cells were seeded on coverslips and fixed with 4% PFA, followed by permeabilization with 0.1% Triton X-100/PBS. After blocking in 3% BSA/PBS, cells were incubated with primary antibodies overnight at 4°C (polyclonal rabbit anti-Zeb1 (Sigma, HPA027524, 1:300); monoclonal mouse anti-E-Cadherin (BD Transduction Laboratories, 610182, Clone 36, 1:200), followed by appropriate Alexa594- and Alexa488-conjugated secondary antibodies (Life technologies) for 1 hour at RT. All images were acquired with a Leica DM5500B microscope and the LAX software (Leica). All IF experiments were performed in at least three individual experiments and one representative image is shown.

Lung colonization/tumourigenicity

Tumour cell colonisation and metastasising capacities to the lung were analysed by tail vein injections into syngeneic mice or NMRI-*Foxn1*$^{nu/nu}$ mice. Primary tumour cell lines were trypsinised and resuspended in appropriate volumes of PBS to inject 200,000 tumour cells in a 200 µl volume using a 27G needle. Mice were sacrificed after 18 days and analysed for

lung metastasis by HE staining. For each cell line three mice were injected and the number or lung metastases were counted on 2 independent sections separated by at least 200 µm. For short-term colonisation analysis cells were infected with pCDH-MSCV-LUC_EF1-GFP-T2A-Puro, selected by puromycin and sorted for medium to high levels of GFP expression. After tail vein injection mice were sacrificed after 2 h. For calculating tumourigenicity and analysis of tumour growth upon subcutaneous engraftment 500, 2,500, 12,500 and 100,000 cells were injected into flanks of C57BL/6 mice. Tumour size was measured 3 times per week and mice were sacrificed if tumours exceeded the size of 500 mm^3 or ulcerated. Tumour initiating frequencies were calculated using the ELDA software (http://bioinf.wehi.edu.au/software/elda/).

Microarray analysis, pre-processing, GSEA and data availability

Gene expression of three epithelial, three mesenchymal KPC, six KPCZ, two TGFβ-treated epithelial KPC and two TGFβ-treated KPCZ cell lines was measured using Illumina Mouse WG6 v2 beadarrays (Illumina, San Diego, CA, USA). Total RNA was isolated, labelled and hybridised according to the manufacturer's protocol in two separate experiments. Raw microarray data were processed and quantile normalised using the Bioconductor R package beadarray[69] and subsequently batch corrected according to their chip identity via ComBat[70] as implemented in the R Bioconductor sva package. Illumina probes were mapped to Entrez IDs using the IlluminaMousev2 annotation (v. 1.26) from Bioconductor. If several probes mapped to the same Entrez ID, the one having the largest interquartile range was retained, which resulted in 20,052 uniquely annotated genes. Gene Set Enrichment analysis (GSEA) was performed using the Broad Institute platform (http://www.broadinstitute.org/gsea/index.jsp; Version 2.2.2). A total of 189 gene sets of the oncogenic signature C6 from the Molecular Signatures database (http://www.broadinstitute.org/gsea/msigdb/genesets.jsp?collection=C6) were used for the analysis with default settings and 1,000 gene set permutations. Additionally 36 gene sets,

related to pancreatic cancer, Zeb1 or metastasis were selected from MSigDB and also analysed (Supplementary Table 4). Gene Sets from classical, quasi-mesenchymal and exocrine-like PDAC subtypes were obtained from Collisson et al. 2011[36].

Metabolic parameters

Bioenergetics of epithelial KPC and KPCZ cell lines was determined using the XFe96 Extracellular Flux Analyzer (Seahorse Bioscience/Agilent Technologies, North Billerica, MA). Cells were seeded in specialised cell culture microplates at a density of 15,000 /well and cultured for 18 h. 1 h before the measurement cells were incubated at 37°C in a CO_2-free atmosphere. For the determination of glycolytic parameters a glycose stress test was performed: basal extracellular acidification rate (ECAR; indicative of glycolysis) was first determined under glucose-free conditions. Secondly, the rate of glycolysis was calculated using the ECAR after glucose supplementation (10 mM). Finally, glycolytic capacity and glycolytic reserve were calculated after inhibition of mitochondrial respiration via oligomycin (Sigma, 75351, 1 µM) and hexokinase activity via 2-deoxy-glucose (2DG, Sigma, D6134, 100 mM).). For the determination of respiratory parameters a mito stress test was performed: basal oxygen consumption rate (OCR, indicator for mitochondrial respiration) was measured. Next, responses toward the subsequent addition of oligomycin (1 µM), FCCP (Sigma, C2920, 1 µM) and the combination of antimycin A (Sigma, A8674, 3 µM) and rotenone (Sigma, R8875, 3 µM) were evaluated allowing for the calculation of basal and maximal respiration as well as respiration-related ATP production. All experiments were performed in heptaplicates.

Statistics and Reproducibility

Statistical analysis was performed using GraphPad Prism software (Version 6.07). Data are represented by means ±SD unless otherwise indicated. For survival analysis the log-rank Mantel-Cox test was used. Tumour/PanIN grading, ECM deposition, local invasion, CD31 and Gata 6 staining, Ki67-positive tumour cell counting, cleaved Casp3-positive tumour cell amounts, PanIN areas, lung colonisation assay and sphere forming capacity analysis were

tested for significance with a two-tailed Mann-Whitney test or an unpaired two-tailed t-test as indicated. A Welch's correction was performed where appropriate. Chi-square analysis was performed to compare frequencies of metastases and number of tumour-initiating cells as well as frequency of Zeb1, Snail, Slug, Twist Zeb2, E-cad and Sox2 positive tumours. Tumour growth, ECAR and OCR were tested for significance at individual time points by a t-test with Holm-Sidak test for multiple comparison. qPCR data were tested for significance with a one-tailed Mann-Whitney test or an unpaired one-tailed t-test as indicated. p-values of statistical significance are represented as: *p<0.05; **p<0.01; ***p<0.001; ****p<0.0001.

Data Availability

Microarray data generated in this study have been deposited in the Gene Expression Omnibus (GEO) under accession code GSE87472. The 189 publically available gene sets reanalysed here were from of the oncogenic signature C6 available from the Molecular Signatures database (http://www.broadinstitute.org/gsea/msigdb/genesets.jsp?collection=C6, Broad Institute, 741 MSigDB, Version 5.1.). The 36 publically available gene sets related to pancreatic cancer, Zeb1 or metastasis were selected from MSigDB and reanalysed here (see also Supplementary Table 4). Gene Sets from classical, quasi-mesenchymal and exocrine-like PDAC subtypes re-analysed here were obtained from Collisson et al. 2011[36]. Source data for Fig. 3c,d,f; Fig. 6d,g and Supplementary Fig. 5d, 7a have been provided as Supplementary Table 5. All other data supporting the findings of this study are available from the corresponding author on reasonable request.

Additional references for methods

62. Olive, K.P. *et al.* Mutant p53 gain of function in two mouse models of Li-Fraumeni syndrome. *Cell* **119**, 847-860 (2004).
63. Jackson, E.L. *et al.* Analysis of lung tumor initiation and progression using conditional expression of oncogenic K-ras. *Genes Dev* **15**, 3243-3248 (2001).
64. Hingorani, S.R. *et al.* Preinvasive and invasive ductal pancreatic cancer and its early detection in the mouse. *Cancer Cell* **4**, 437-450 (2003).

65. Chan, I.T. *et al.* Conditional expression of oncogenic K-ras from its endogenous promoter induces a myeloproliferative disease. *J Clin Invest* **113**, 528-538 (2004).
66. Novak, A., Guo, C., Yang, W., Nagy, A. & Lobe, C.G. Z/EG, a double reporter mouse line that expresses enhanced green fluorescent protein upon Cre-mediated excision. *Genesis* **28**, 147-155 (2000).
67. Murray, S.A., Carver, E.A. & Gridley, T. Generation of a Snail1 (Snai1) conditional null allele. *Genesis* **44**, 7-11 (2006).
68. Meidhof, S. *et al.* ZEB1-associated drug resistance in cancer cells is reversed by the class I HDAC inhibitor mocetinostat. *EMBO molecular medicine* **7**, 831-847 (2015).
69. Dunning, M.J., Smith, M.L., Ritchie, M.E. & Tavare, S. beadarray: R classes and methods for Illumina bead-based data. *Bioinformatics* **23**, 2183-2184 (2007).
70. Johnson, W.E., Li, C. & Rabinovic, A. Adjusting batch effects in microarray expression data using empirical Bayes methods. *Biostatistics* **8**, 118-127 (2007).

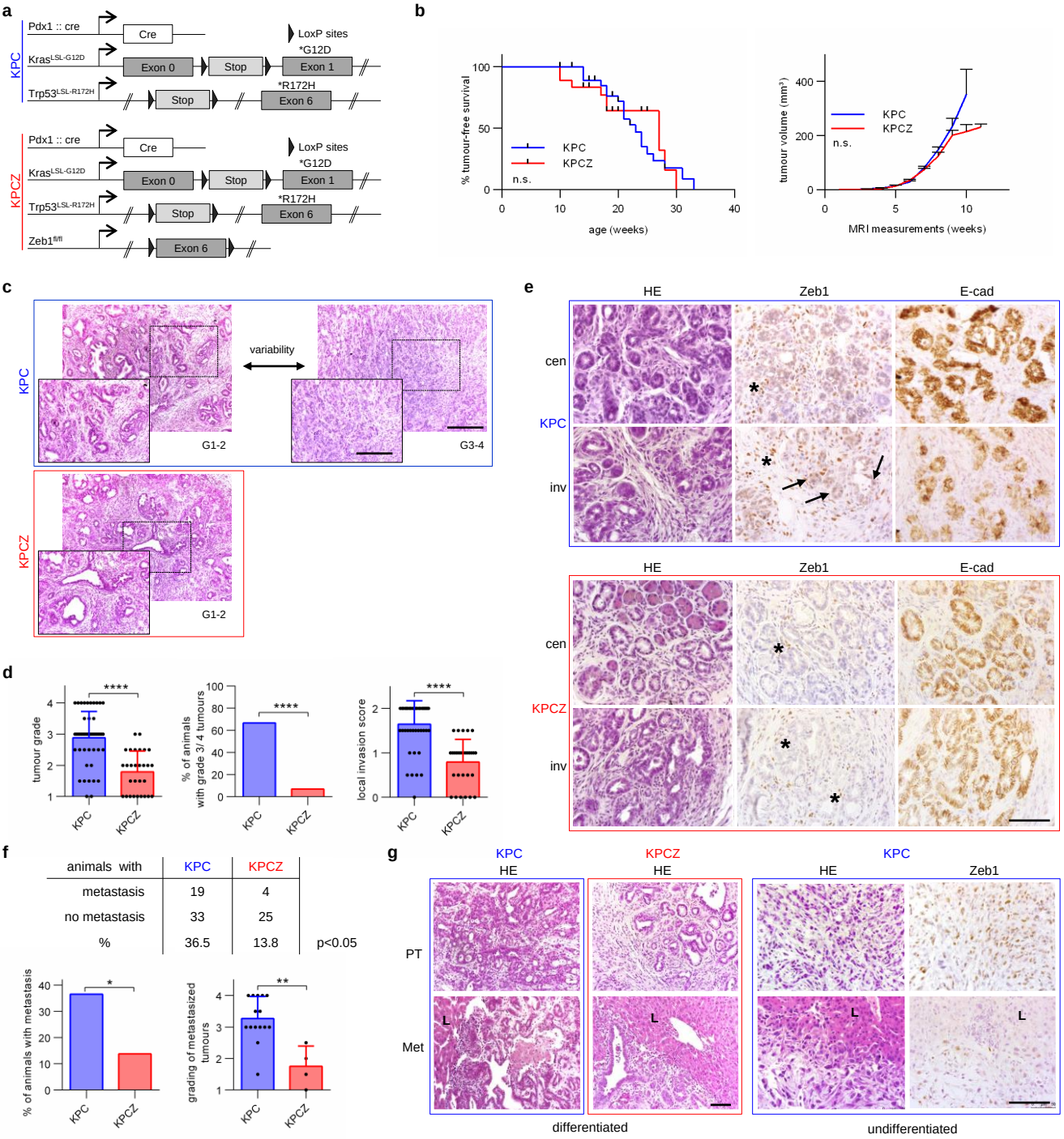

Krebs et al. Fig. 1

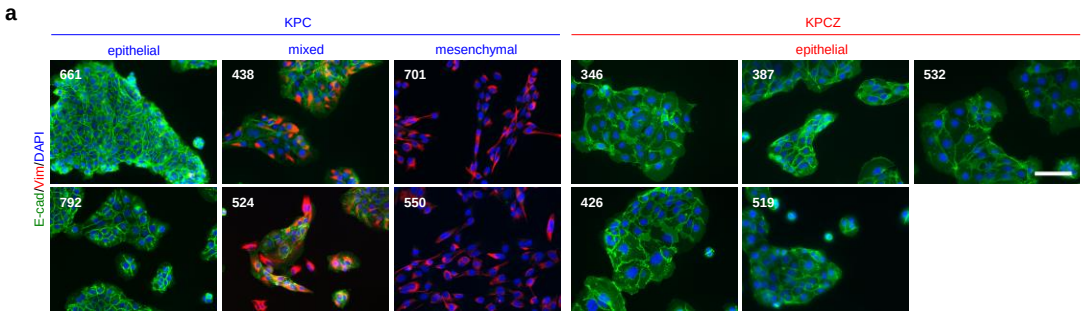

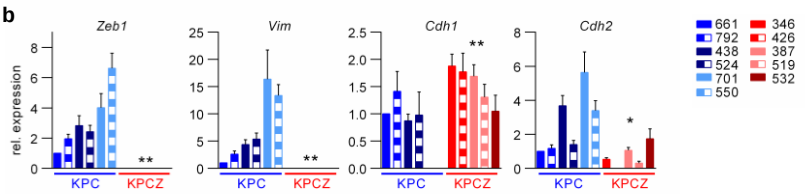

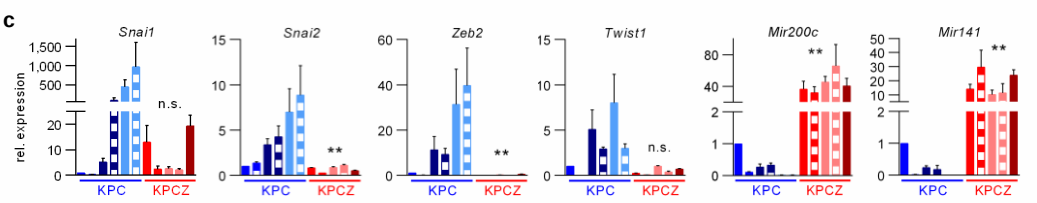

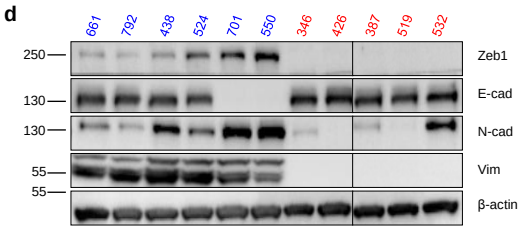

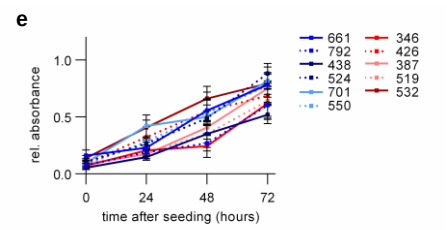

Krebs et al. Fig. 2

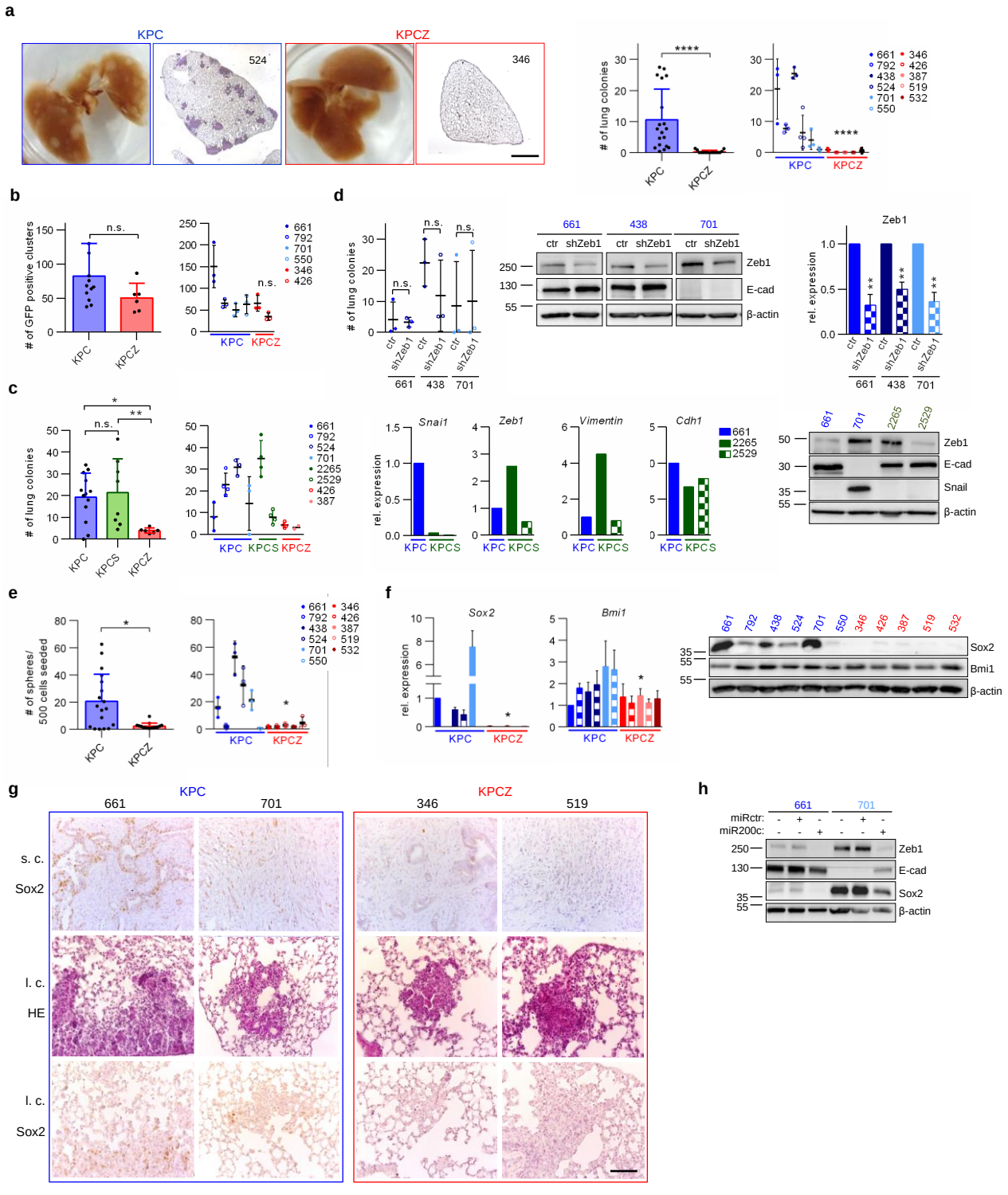

Krebs et al. Fig. 3

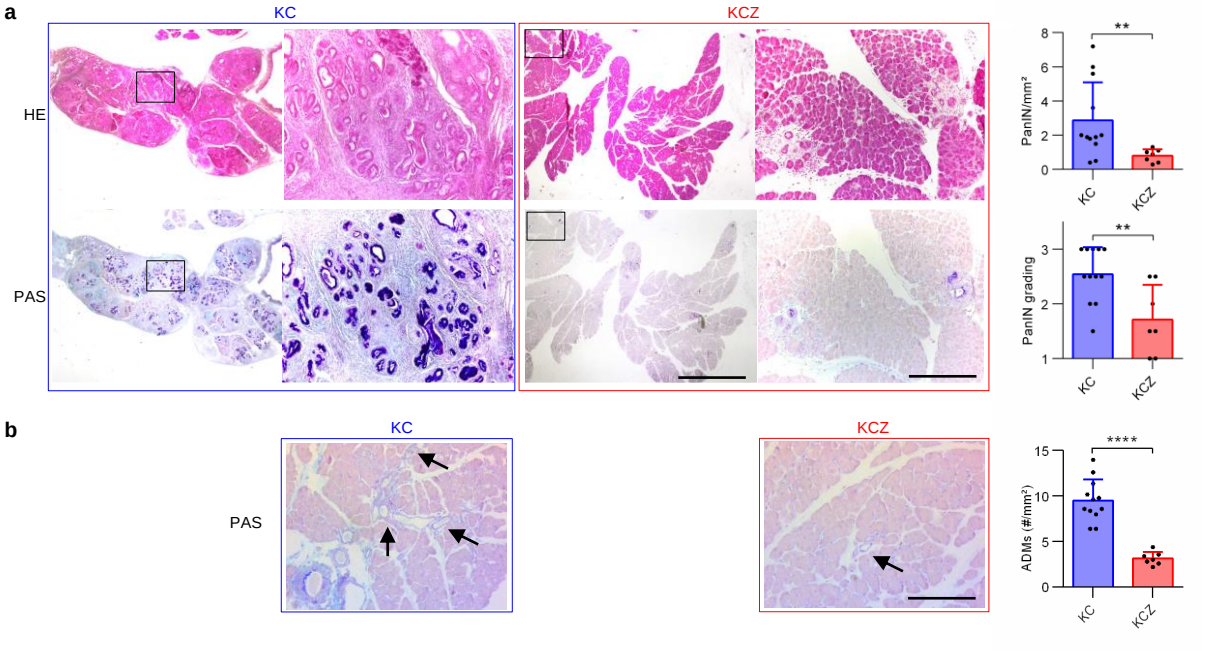

Krebs et al. Fig. 4

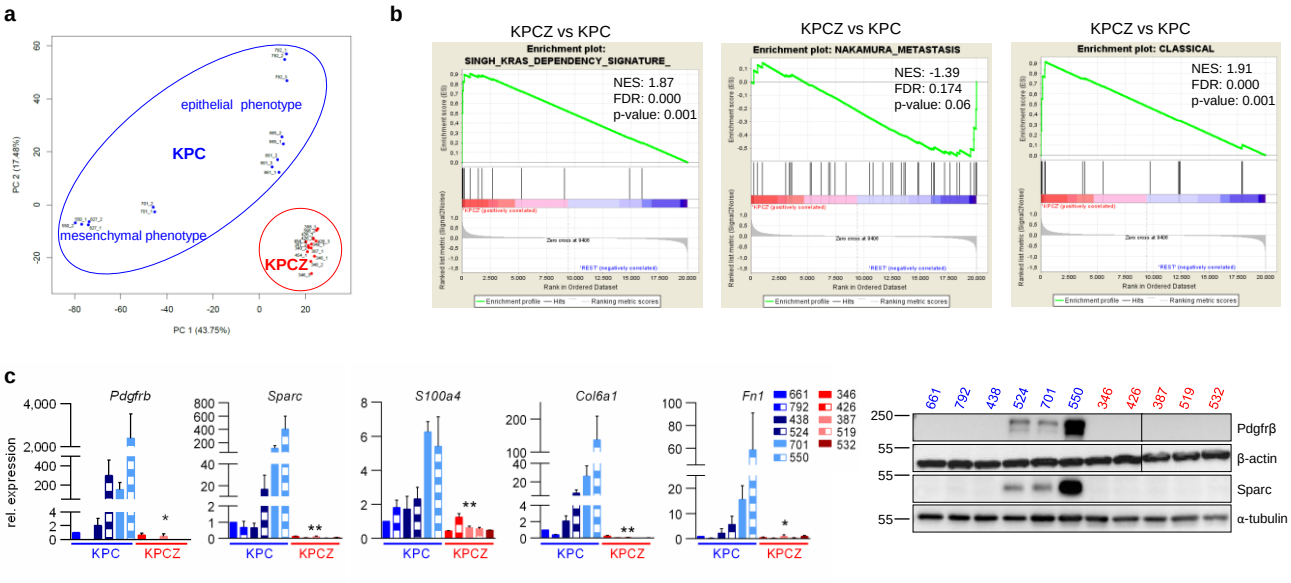

Krebs et al. Fig. 5

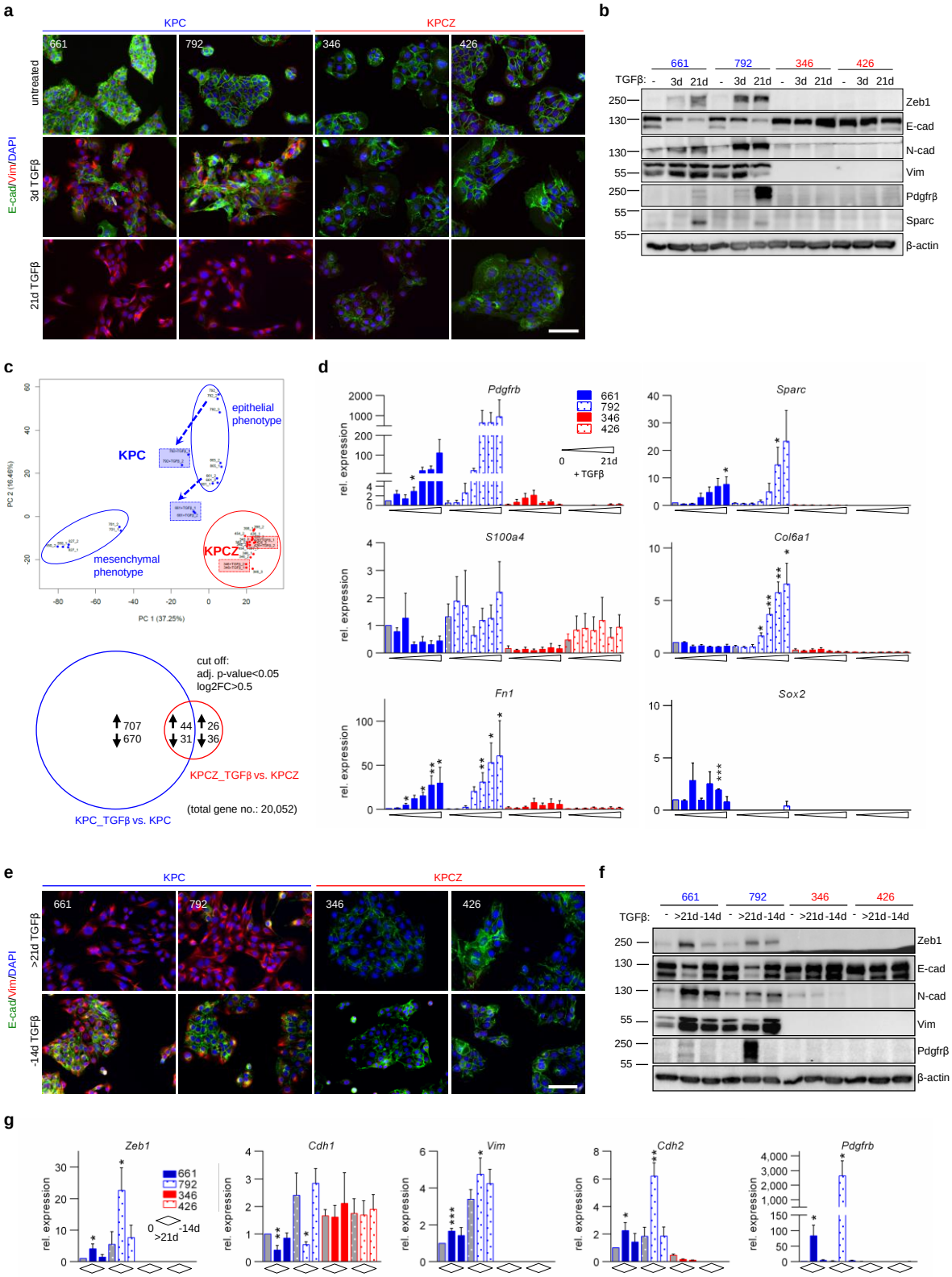

Krebs et al. Fig. 6

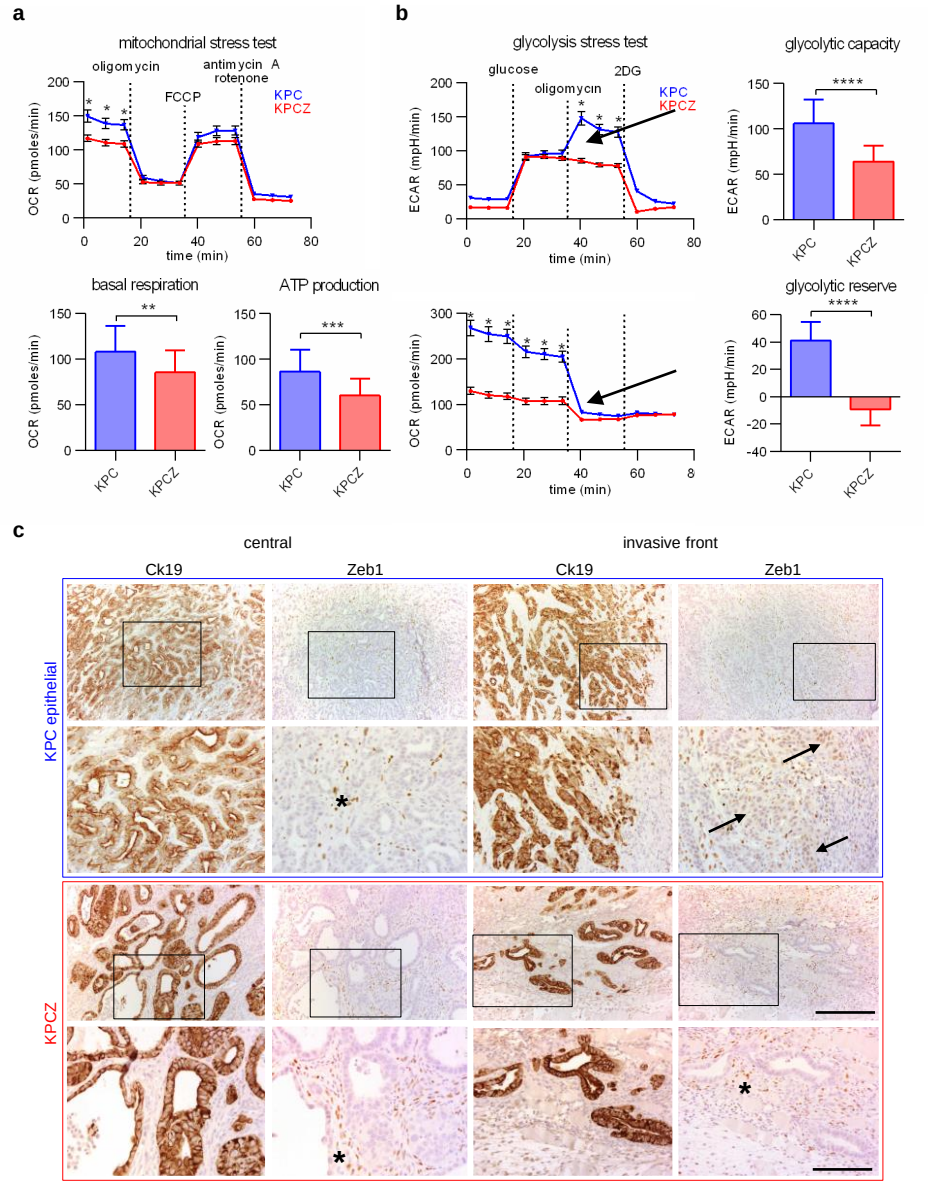

Krebs et al. Fig. 7

genotype	phenotype	cell line	sphere formation	tumourigenicity	plasticity	lung colonisation	lung dissemination
KPC	epithelial	661	++	+++	+++	+++	+++
		792	+	+++	+++	+	++
	mesenchymal	701	++	++	na	+	++
		550	-	+	na	-	++
KPCZ	epithelial	346	-	+	-	-	++
		426	-	+	-	-	++

Krebs et al. Table 1